Asian Journal of Chemistry; Vol. 26, No. 15 (2014), 4901-4906

ASIAN JOURNAL OF CHEMISTRY

http://dx.doi.org/10.14233/ajchem.2014.17024

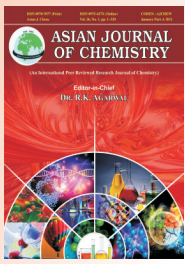

Adsorption Behaviour of Reduced Graphene Oxide for Removal of Heavy Metal Ions

BO WANG, FAN ZHANG*, SHENGFU HE, FU HUANG and ZHIYUAN PENG

College of Chemistry and Chemical Engineering, Jishou University, Jishou 416000, P.R. China

*Corresponding author: Tel/Fax: +86 743 8563911; E-mail: zhangfan8346@sina.com

Received: 11 January 2014; *Accepted*: 13 February 2014; *Published online*: 16 July 2014; AJC-15596

Reduced graphene oxide was prepared by reducing graphene oxide with ethylenediamine. The adsorption behavior of the reduced graphene oxide for Pb(II), Cd(II), Cu(II) and Mn(II) was studied and the effects of media pH, adsorption time and initial metal ion concentration on adsorption capacity of the adsorbent were investigated. The adsorption capacities of reduced graphene oxide were found to be 413.22, 162.33, 55.34 and 42.46 mg/g for Pb(II), Cd(II), Cu(II) and Mn(II), respectively and the adsorption reaches equilibrium within 60 min. Experimental data were exploited for kinetic evaluations related to the adsorption processes. Adsorption kinetic data can be satisfactorily described by the pseudo-second-order equation and the Langmuir adsorption model agrees well with the experimental data. The adsorption capacity of reduced graphene oxide for Pb(II) decreased not more than 20 % for the three cycles, indicating the feasibility of reduced graphene oxide adsorbent in metal recovery and removal.

Keywords: Reduced graphene oxide, Adsorption, Heavy metal ions.

INTRODUCTION

As one of the most promising techniques for removal or selectively recovery of heavy metals from the industrial effluents, the adsorption technology has been employed for many years and various adsorbents have been studied, including activated carbon[1-3], chitosan[4-6], kaolinite[7-9], diatomite[10-12], zeolite[13-15], silica gel[16,17], alumina[18,19], functionalized polymers[20-22], zero-valent iron[23,24] and nanomaterials[25]. However, most of these adsorbents are not the ideal choices for their unsatisfied adsorption capacity, insufficient adsorption efficiencies, or high price in application.

Recently, graphene and graphene composites have been studied extensively for several applications including the adsorption for the removal and recovery of metal ions[26-38]. Chang *et al.*[39] reported the synthesis of graphene sheets by ionic-liquid-assisted electrolysis and its adsorption for Fe(II) with a capacity of 299.3 mg/g. Fan *et al.*[40] investigated the adsorption properties for Pb(II) of the magnetic chitosan grafted with graphene oxide sheets. Mi *et al.*[41] reported the synthesis of graphene oxide areogels by a unidirectional freeze-drying method and their adsorption performance for Cu(II) in aqueous solution.

In this paper, the graphene oxide was reduced by ethylenediamine according to Che's method[42] and the reduced graphene oxide was characterized by Fourier transform infrared spectra (FT-IR), Raman spectra, thermogravimetric analysis (TGA) and atom force microscopy (AFM). The purpose of this work is to combine the features of graphene oxide with ethylenediamine, *i.e.*, the reduced graphene oxide contained carboxyl and amino group simultaneously. The adsorption behavior of the reduced graphene oxide for Pb(II), Cd(II), Cu(II) and Mn(II) was studied. Various factors influencing the adsorption of Pb(II), Cd(II), Cu(II) and Mn(II), *e.g.* pH, contact time and adsorbate concentration were investigated and the regeneration of the adsorbent was also studied. To the best of our knowledge, the literatures were scarcely reported about the application of the reduced graphene oxide which combined both features of the carboxyl and amino groups for removal and recovery of heavy metals in aqueous solutions.

EXPERIMENTAL

Graphite powder (Tianjin Kemiou Chemical Reagent Co., Ltd., Tianjin, China) was of analytical grade. ethylenediamine (Tianjin Fuyu Fine Chemical Co., Ltd., Tianjin, China) was of analytical grade. $Pb(NO_3)_2$, $Cd(NO_3)_2$, $CuSO_4{\cdot}5H_2O$, $MnSO_4{\cdot}H_2O$ and the other chemicals used were all of commercial analytical grade and were purchased from Tianjin Kemiou Chemical Reagent companies.

Preparation of graphene oxide: Graphene oxide was prepared by a modified Hummers method[43]. Under ice bath, graphite powder (2.5 g), $NaNO_3$ (2.5 g) and concentrated H_2SO_4 (115 mL) were stirred together and then $KMnO_4$ (15 g) was slowly added. Once mixed, the solution was transferred to a 35 ± 5 °C water bath and stirred for 1 h. Then, the distilled

water (200 mL) was slowly added, the solution was stirred at 90 ± 5 °C for 0.5 h. And then, the distilled water (500 mL) was added, followed by adding 15 mL H_2O_2 (30 %), the color of the solution turned from dark brown to bright yellow. Followed, the warm solution was then filtered and washed with the distilled water. High-speed centrifugation was done at 8000 rpm for 0.5 h. It was repeated until the solution was neatly neutral. Then the distilled water inside the solution was replaced by DMF. Finally, graphene oxide dispersion in DMF was sonicated for 1 h by using a ultrasonic cleaner.

Preparation of reduced graphene oxide: Reduced graphene oxide was prepared according to the reported literature[42]. Graphene oxide (2 g) was dissolved in DMF in a three-necked round-bottomed flask. Then ethylenediamine (20 mL) was added into the flask dropwise and the solution was refluxed under 80 °C for 24 h. The resultant product was filtered and washed with DMF. The colloidal sediment was dried under vacuum at 100 °C for 12 h and the reduced graphene oxide was prepared.

Characterization of reduced graphene oxide: The reduced graphene oxide was analyzed by FT-IR (Nicolet iS10, Thermo Fisher Scientific) using KBr pellets in the 4000-500 cm^{-1} region. TGA (TGA/DSC1, Mettler Toledo) measurement was performed under nitrogen atmosphere from 40 to 800 °C at a heating rate 10 °C/min. Raman spectra were obtained using a confocal microprobe Raman system (Renishaw, RM 2000). AFM (SPA 400) image was obtained under ambient in tapping mode. The N_2-based Brunaer Emmett Teller (BET) surface area and pore-size distribution of reduced graphene oxide were determined by the Surface Area Analyzer (NOVA4200e, Quantachrome). The concentrations of metal ions were determined by an atomic absorption spectrometer (AA-6300C, Shimadzu). The zeta potential of reduced graphene oxide was measured using a ζ-sizer (Nano ZS-90, Malvern). The pH values of metal ion solutions were measured with a PHSJ-4A pH meter (Shanghai Precision Science Equipment Co. Ltd.).

Adsorption kinetics experiments: 800 mL of metal ions solution of 200 mg/L was placed into a round-bottomed flask of 2000 mL, reduced graphene oxide (0.1 g) was added into the flask and stirred under water bath at 25 °C. Then 5 mL of this solution was taken out for filtrating at different time intervals. The concentrations of metal ions were determined by using atomic absorption spectrometer (AAS). The amount of metal ions adsorbed by reduced graphene oxide was calculated according to the following eqn. 1:

$$Q = \frac{(C_0 - C) \times V}{W} \quad (1)$$

where Q is the amount of metal ions adsorbed onto unit amount of the reduced graphene oxide (mg/g), C_0 and C are the initial and equilibrium concentrations of the metal ions in aqueous phase (mg/L), respectively. V is the volume of the aqueous phase (L) and W is the dry weight of the adsorbent (g).

Isothermal adsorption experiments: 100 mL of metal ions solution with different concentration was placed into round-bottomed flask of 250 mL and reduced graphene oxide (0.1 g) was added into these solutions, respectively. After ultrasonic treatment for 1 h, the flask was transferred to water bath and stirred for 4 h at 25 °C. With the funnel filtering, the equilibrium concentrations of metal ions were determined by using AAS. The amount of metal ions adsorbed by reduced graphene oxide was calculated according to eqn. 1.

Regeneration: The reduced graphene oxide (0.1 g) was mixed with 414 mg/L Pb(II) solution for 4 h, then the adsorbent was washed with excess of distilled water after adsorption and 0.05 M HCl solution was applied to elute. Washed with excess of distilled water, the adsorbent was mixed with 414 mg/L Pb(II) solution for 4 h again, the equilibrium concentrations of metal ions were determined by using AAS, the adsorption capacity was obtained according to eqn. 1.

RESULTS AND DISCUSSION

Characterization of reduced graphene oxide: Fig. 1a presented the FTIR spectra of graphene oxide and reduced graphene oxide. The band at 1728 cm^{-1} was associated with stretching of the C=O bond of carbonyl or carboxyl groups for graphene oxide and an intense band at 1230 cm^{-1} was observed which is attributed to the stretching of the C-O bond. There was a new broad band at 1540 cm^{-1} which was associated with the vibration of N-H groups. The strong absorption at 3430 cm^{-1} can be associated with N-H and O-H stretching vibration, demonstrating the successful chemical reaction between graphene oxide and ethylenediamine. Fig. 1b presented the Raman spectra of graphite, graphene oxide and reduced graphene oxide. Raman spectra of graphite displayed a typical G peak at 1579 cm^{-1}. In Raman spectra of graphene oxide, the G band was broadened and shifted to 1592 cm^{-1}. The Raman spectra of the reduced graphene oxide also contained both G and D band at 1584 and 1346 cm^{-1}, respectively and the ratio of I_D and I_G increased from 1.05 (graphene oxide) to 1.08 (reduced graphene oxide) slightly. This change suggested a decrease in the average size of the sp^2 domains upon reduction of graphene oxide. As described in Fig. 1c, graphene oxide decomposed heavily at the temperature of 187.1 °C. It was caused by the pyrolysis of the oxygen-containing functional groups, forming CO, CO_2 and H_2O[44]. After being functionalized by the amine groups, the decomposition temperature of reduced graphene oxide increased in a certain extent compared with graphene oxide. Also, the TGA curve of reduced graphene oxide exhibited a slight weight loss at the temperature lower than 210 °C suggesting that graphene oxide was reduced, which showed a better thermal stability[45]. As shown in Fig. 1d, AFM was used to further identify the monolayer structure of reduced graphene oxide sheet. The sheet with a thickness of 0.69 nm was observed, this can be regarded as the monolayer reduced graphene oxide sheet[46]. The BET specific surface area of reduced graphene oxide is 28 m^2/g which was much lower than that of previous graphene oxide sample data[42]. This might be due to the incomplete exfoliation of graphene oxide and the agglomerations occurred during reduction process[47].

Effect of pH on the removal of metal ions: The adsorption performances of reduced graphene oxide for metal ions at different solution pH values were shown in Fig. 2. As showed in Fig. 2, the adsorption capacity for heavy metal ions was increased with increasing solution pH. Below pH of 3, the H_3O^+ ions of higher concentration will compete with M(II) to

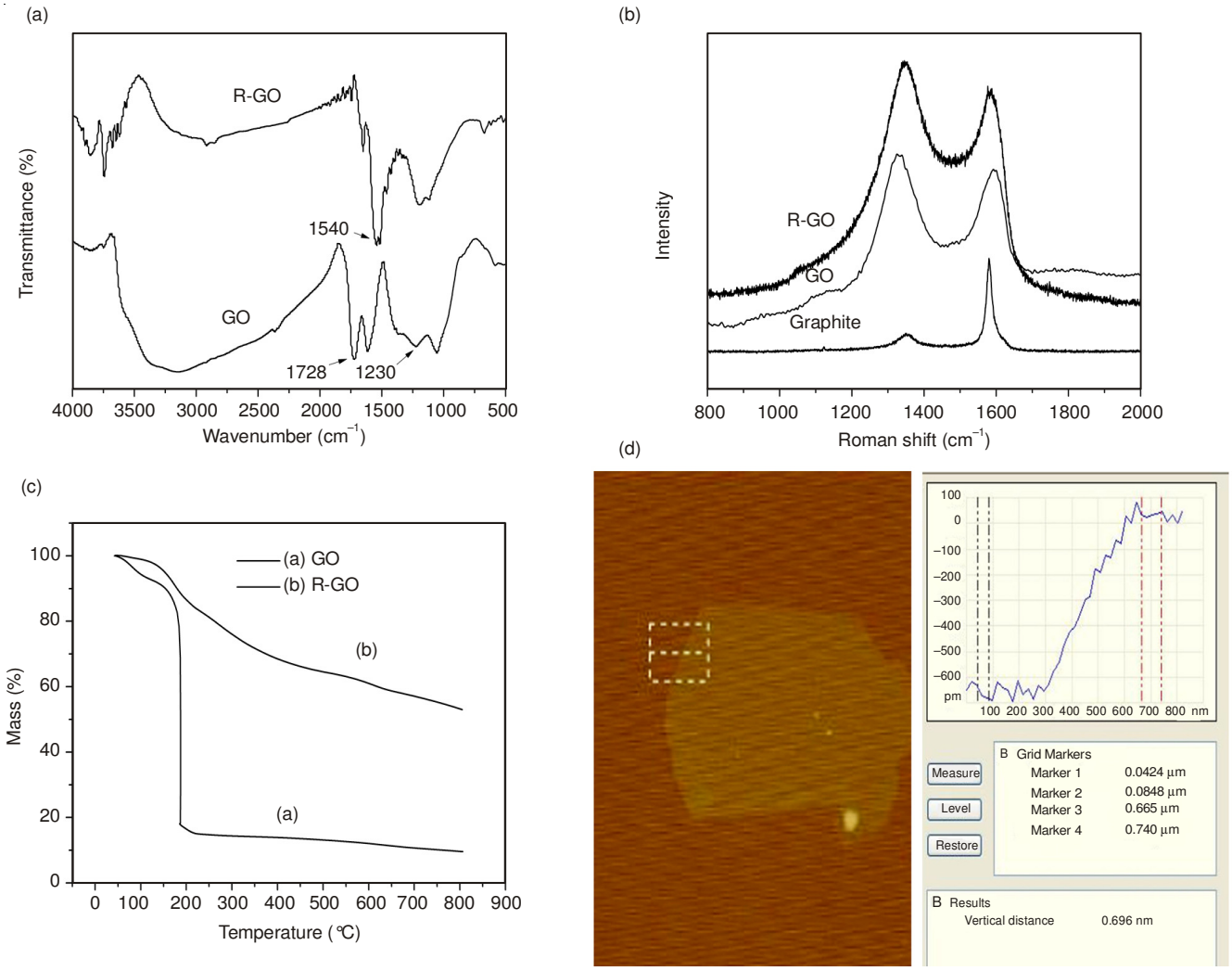

Fig. 1. (a) FT-IR spectra of graphene oxide and reduced graphene oxide, (b) Raman spectra of graphite, graphene oxide and reduced graphene oxide, (c) TGA curves of graphene oxide and reduced graphene oxide and (d) AFM image of reduced graphene oxide

seize the adsorption sites[48] and as a result, less adsorption capacities were observed at low pH. With the pH increased, the protonation degree of the amino groups weakened and the coordination and chelating ability of these amino groups towards Pb(II), Cd(II), Cu(II) and Mn(II) strengthened. But at pH higher than 4.5, the adsorption capacity for heavy metal ions decreased in a way because heavy metal ions might precipitate. In addition, the active adsorption sites mainly turned into dissociated forms, which resulted in the high affinity of adsorption sites towards the metal ions[49]. Results of Zeta potential measurement for reduced graphene oxide at different pH are shown in Fig. 3. Zeta potentials of the reduced graphene oxide decreased with increasing pH. The PZCs were estimated at pH 7 for reduced graphene oxide. It was obvious that in the pH ranges, reduced graphene oxide surface is positively charged. With the pH increased, the adsorption capacity of reduced graphene oxide for heavy metal ions increased and the numbers of positive charge on reduced graphene oxide decreased. Then it might be that the electrostatic attraction between reduced graphene oxide and heavy metal ions was weak relatively and with the repulsion between heavy metal ions and positive charge on reduced graphene oxide weakened, the chelating ability of amino groups towards heavy metal ions strengthened, which contribute to the increase of the adsorption capacity of reduced graphene oxide for heavy metal ions.

The optimum pH value at which the maximum metal uptake were obtained as 4.5, 5.0, 4.5 and 5.0 for Pb(II), Cd(II), Cu(II) and Mn(II), respectively. These optimum pH values were used for experiments followed.

Adsorption kinetics: Fig. 4a shows the kinetic curves of Pb(II), Cd(II), Cu(II) and Mn(II) onto reduced graphene oxide. It can be seen that the adsorption of Pb(II), Cd(II), Cu(II) and Mn(II) onto reduced graphene oxide increases sharply within the first 0.5 h, then it rises slowly and reaches equilibrium in 1 h. The process of adsorption achieved equilibrium in such a short time, suggested that reduced graphene oxide had very high adsorption efficiency and high-value industrial applications.

In order to interpret the kinetic characteristics of metal adsorption processes, the pseudo-first-order[50] and pseudo-second-order[51] kinetic models have been employed to fit the experimental data in this work. The pseudo-first-order kinetic model was generally expressed as the equation:

$$-\ln\left(1-\frac{Q_t}{Q_e}\right) = k_1 t + C \text{ , } F = Q_t/Q_e \qquad (2)$$

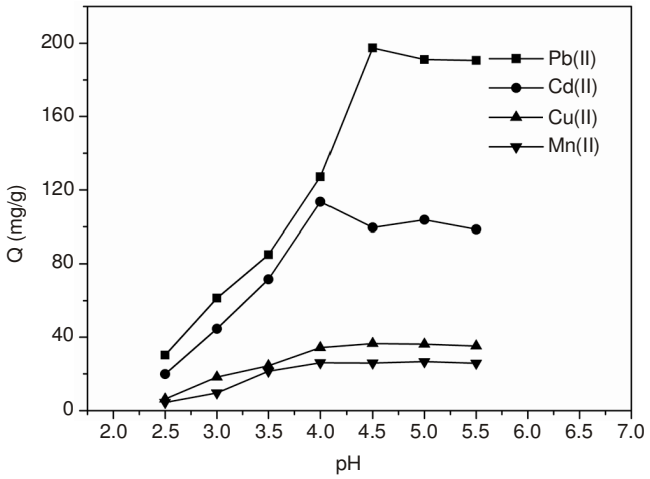

Fig. 2. Influence of pH on the adsorption capacity temperature: 25 °C; adsorption time: 4 h. reduced graphene oxide 0.1 g, Pb(II) 414 mg/L, Cd(II) 224 mg/L, Cu(II) 128 mg/L and Mn(II) 110 mg/L; 0.1 L

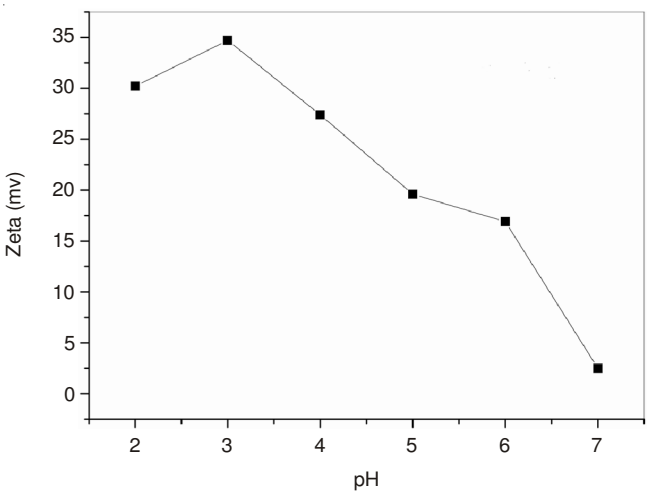

Fig. 3. Zeta potentials of reduced graphene oxide different pH conditions

where Q_e and Q_t are the amounts of the metal ions adsorbed (mg/g) at equilibrium and at contact time t (min), respectively, k_1 (1/min) is the rate constant. The plots of -ln(1-F) *versus* t were shown in Fig. 4b.

The experimental data were also fitted by the pseudo-second-order kinetic model which was given with the equation below:

$$\frac{t}{Q_t} = \frac{1}{k_2 Q_e^2} + \left(\frac{1}{Q_e}\right)t \quad (3)$$

where k_2 (g/mg min) is the rate constant of pseudo-second-order adsorption reaction. The plots of t/Q_t *vs.* t were shown in Fig. 4c and the rate constants (k_2) were presented in Table-1.

TABLE-1
FIRST-ORDER, SECOND-ORDER RATE CONSTANTS

Metal	First-order rate constants			Second-order rate constants		
	Q_e (mg/g)	k_1 (1/min)	R^2	k_2 (g/mg min)	Q_e (mg/g)	R^2
Pb(II)	199.82	0.00887	0.8848	0.00403	200.8	0.9999
Cd(II)	89.95	0.01001	0.9853	0.00285	90.5797	0.9999
Cu(II)	39.87	0.01746	0.8947	0.00061	44.5831	0.9965
Mn(II)	22.36	0.01166	0.9298	0.00173	24.2895	0.9991

From Table-1, the R^2 values of the pseudo-first-order kinetic model for the adsorption of Pb(II), Cd(II), Cu(II) and Mn(II) onto reduced graphene oxide were 0.8848, 0.9853, 0.8947 and 0.9298 and those of pseudo-second-order kinetic model were 0.9999, 0.9999, 0.9965 and 0.9991. It indicated that pseudo-second-order kinetic model provided a better correlation in contrast to the pseudo-first-order model for adsorption of Pb(II), Cd(II), Cu(II) and Mn(II) onto reduced graphene oxide. It was possible to suggest that the adsorption of Pb(II), Cd(II), Cu(II) and Mn(II) followed a second-order type reaction kinetics. The pseudo-second-order model was based on the assumption that the rate-determining step might be a chemical adsorption involving valence forces through sharing or exchanging of electrons between adsorbent and adsorbate[49,52].

Adsorption isotherms: The adsorption isotherms of reduced graphene oxide for different metal ions were shown in Fig. 5. When the initial concentration of the metal ions increased from 1 to 6 mmol/L, the adsorption capacity of reduced graphene oxide at 25 °C for Pb(II), Cd(II), Cu(II) and Mn(II) increased in the range of 173.41-396.63, 41.11-115.25, 38.94-54.17 and 22.97-38.61 mg/g, respectively. Obviously, the adsorption capacity followed the order of Pb(II) > Cd(II) > Cu(II) > Mn(II). These results indicated that the adsorption was not only due to the carboxyl group but also the amino group in the reduced graphene oxide and the reduced graphene oxide had higher affinity to Pb(II) than Cd(II), Cu(II) or Mn(II).

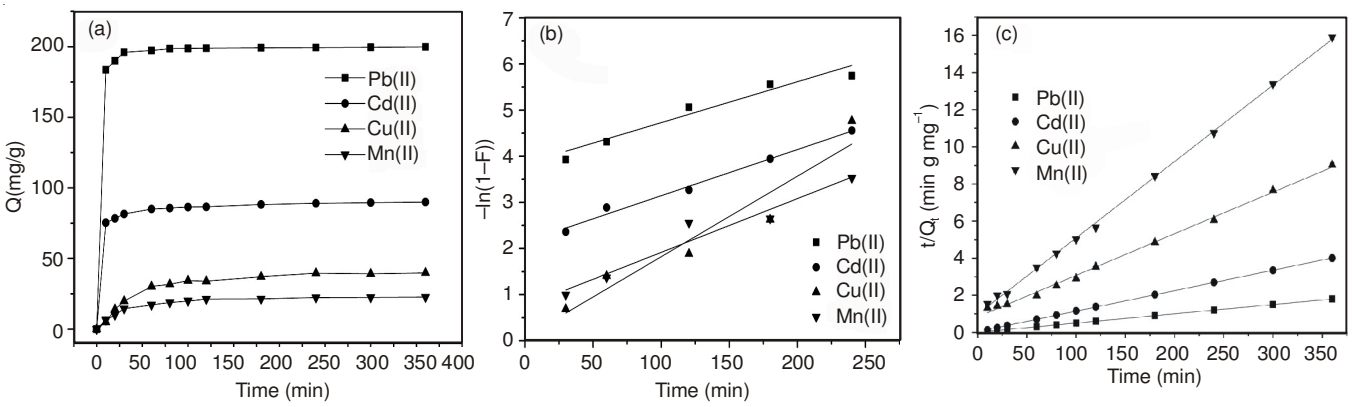

Fig. 4. (a) Kinetic adsorption curve of reduced graphene oxide for metal ions temperature: 25 °C; Pb(II), pH = 4.5; Cd^{2+}, pH = 4; Cu^{2+}, pH = 4.5; Mn^{2+}, pH = 5. (b) Simulated pseudo-first-order kinetics; (c) Simulated pseudo-second-order kinetics

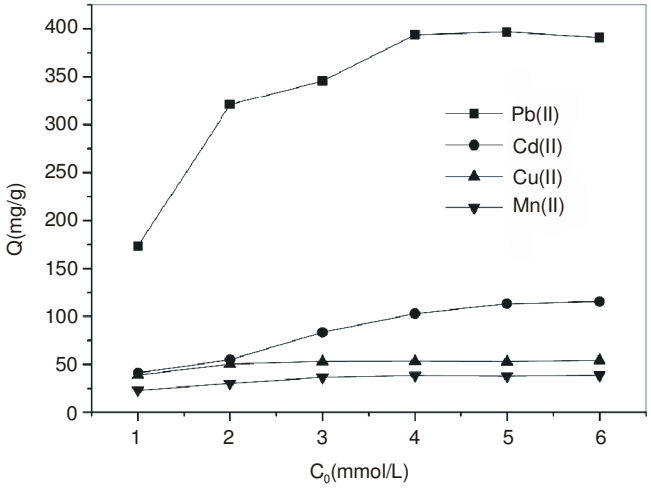

Fig. 5. Adsorption isotherms of reduced graphene oxide for metal ions temperature: 25 °C; adsorption time: 4 h; Pb(II), pH = 4.5; Cd(II), pH = 4; Cu(II), pH = 4.5; Mn(II), pH = 5

The adsorption data for heavy metal ions were analyzed by fitting the Langmuir and Freundlich adsorption isotherm models.

TABLE 2
RELATED CONSTANT AND LINEAR REGRESSION COEFFICIENT OF LANGMUIR-FREUNDLICH FITTING

Fitting model		Adsorbate			
		Pb(II)	Cd(II)	Cu(II)	Mn(II)
Langmuir	Q_m(mg/g)	413.22	162.33	55.34	42.46
	b(L/mg)	0.0267	0.0046	0.1149	0.0382
	R^2	0.9976	0.9868	0.9994	0.9964
Freundlich	k(mg/g)	89.9469	4.4781	27.7293	10.2868
	n	4.2766	1.9026	8.2243	4.0946
	R^2	0.7823	0.9810	0.8119	0.9063

The Langmuir adsorption equation[53] was as follows:

$$Q_e = Q_m \frac{bC_e}{1 + bC_e} \quad (4)$$

$$\frac{C_e}{Q_e} = \frac{C_e}{Q_m} + \frac{1}{bQ_m} \quad (5)$$

where Q_m (mg/g) is the maximum adsorption capacity of metal ion per unit weight of adsorbent; b represents the equilibrium constant of adsorption reaction (L/mg). The values of Q_m and b were presented in Table-2.

The Freundlich adsorption equation[54] and its logarithmic form were as follows:

$$Q_e = kC_e^{1/n} \quad (6)$$

$$\ln Q_e = \ln k + \frac{1}{n} \ln C_e \quad (7)$$

where k and n are the Freundlich constants. k is roughly an indicator of the adsorption capacity (mg/g) and 1/n is an empirical parameter relating the adsorption intensity. The values of k and n were presented in Table-2.

As shown in Table-2, the linear correlation coefficients (R^2) values of Langmuir isotherms were 0.9976, 0.9868, 0.9994 and 0.9964 for Pb(II), Cd(II), Cu(II) and Mn(II) adsorption onto reduced graphene oxide, respectively. These results indicated that the adsorption experimental data of Pb(II), Cd(II), Cu(II) and Mn(II) onto reduced graphene oxide fitted the Langmuir model well. In addition, it can be calculated from the fitting results that the adsorption capacity Q_m of Pb(II), Cd(II), Cu(II) and Mn(II) onto reduced graphene oxide were 413.22, 162.33, 55.34 and 42.46 mg/g, respectively. As showed in Table-2, the adsorption capacity of Pb(II) onto reduced graphene oxide was far more than that of Cd(II), Cu(II) or Mn(II). Therefore, it might be concluded that reduced graphene oxide possessed much superior adsorption ability and higher affinity for Pb(II) than Cd(II), Cu(II) or Mn(II).

The R^2 values of Freundlich isotherms were in the range 0.7823-0.9810 (Table-2), which indicated that the adsorption processes did not fit well with Freundlich model. Hence, the Langmuir model gave the better fit to the experimental equilibrium data. Also, the R^2 values were very close to 1, which indicated that the adsorption of reduced graphene oxide for metal ions was a typical monomolecular layer adsorption.

Regeneration: From an economical point of view, the regeneration capability of adsorbent is an important concern in practical applications. Because the regeneration process could not only restore the adsorption capacity of exhausted adsorbent but also recover valuable components present in the adsorbed phase. Since the adsorption of Pb(II) was highly pH dependent, the desorption of Pb(II) was possible by controlling the pH. In this study, 0.05M HCl was used to ensure a complete detachment of the loaded Pb(II) into washing solution. The Pb(II) adsorption capacity of reduced graphene oxide undergoing three cycles was shown in Fig. 6. The results showed that the adsorption capacity for Pb(II) decreased not more than 20 % for the three cycles, which indicated the feasibility of reduced graphene oxide adsorbent in metal recovery and removal.

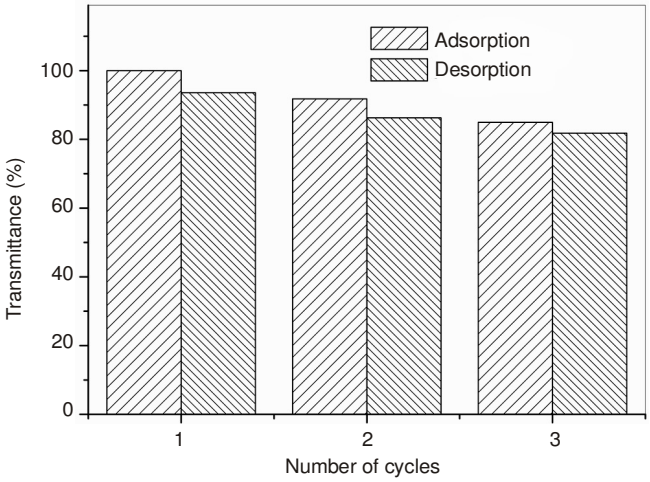

Fig. 6. Adsorption/desorption efficiency of the reduced graphene oxide towards Pb(II) (reduced graphene oxide 0.1 g, HCl C_0 = 0.05 mol/L, contact time 4 h, temperature 25 °C

Conclusion

In presented study, the reduced graphene oxide has been prepared and characterized. The adsorption capacity of the reduced graphene oxide for the heavy metal ions was highly pH dependent. The adsorption process for the heavy metal ions for reduced graphene oxide can be explained with pseudo-

second-order type kinetic model, which is based on the assumption that the rate-determining step is a chemical adsorption. The adsorption of all the metal ions on reduced graphene oxide fits the Langmuir equation well. The maximum adsorption capacity of reduced graphene oxide for Pb(II) is found to be 413.22 mg/g, which is higher than that for Cd(II), Cu(II) or Mn(II). The adsorption reaches equilibrium state within 1 h. On the other hand, the regeneration studies for Pb(II) demonstrated that reduced graphene oxide could be recycled for further use and Pb(II) ion could be separated. The above results indicated that reduced graphene oxide has excellent adsorption properties for removing heavy metal ions from wastewater.

ACKNOWLEDGEMENTS

The work was supported by Natural Science Foundation of Hunan Province (No. 11JJ3053), Key Science and Technology Financing Projects of Ministry of Education (No. 211124) of China, Scientific Research Fund of Hunan Provincial Education Department (No. 10B087), National Natural Science Foundation of China (31360161).

REFERENCES

1. H. Trevino-Cordero, L.G. Juárez-Aguilar, D.I. Mendoza-Castillo, V. Hernández-Montoya, A. Bonilla-Petriciolet and M.A. Montes-Morán, *Ind. Crops Prod*., **42**, 315 (2013).
2. C. Faur-Brasquet, K. Kadirvelu and P. Le Cloirec, *Carbon*, **40**, 2387 (2002).
3. J. Rivera-Utrilla, I. Bautista-Toledo, M.A. Ferro-García and C. Moreno-Castilla, *Carbon*, **41**, 323 (2003).
4. A. Shafaei, F.Z. Ashtiani and T. Kaghazchi, *Chem. Eng. J*., **133**, 311 (2007).
5. D. Kolodynska, *Chem. Eng. J*., **173**, 520 (2011).
6. A.H. Chen, S.C. Liu, C.Y. Chen and C.Y. Chen, *J. Hazard. Mater*., **154**, 184 (2008).
7. S. Sen Gupta and K.G. Bhattacharyya, *J. Environ. Manag*., **87**, 46 (2008).
8. P. Srivastava, B. Singh and M. Angove, *J. Colloid Interf. Sci*., **290**, 28 (2005).
9. M.Q. Jiang, X.Y. Jin, X.Q. Lu and Z.L. Chen, *Desalination*, **252**, 33 (2010).
10. N. Caliskan, A.R. Kul, S. Alkan, E.G. Sogut and I. Alacabey, *J. Hazard. Mater*., **193**, 27 (2011).
11. S. Yusan, C. Gok, S. Erenturk and S. Aytas, *Appl. Clay Sci*., **67-68**, 106 (2012).
12. M. Gürü, D. Venedik and A. Murathan, *J. Hazard. Mater*., **160**, 318 (2008).
13. L. Zhang, H. Zhang and X. Yu, *Water Environ. Res*., **83**, 2170 (2011).
14. I.W. Nah, K.Y. Hwang, C. Jeon and H.B. Choi, *Miner. Eng*., **19**, 1452 (2006).
15. W. Qiu and Y. Zheng, *Chem. Eng. J*., **145**, 483 (2009).
16. E. Bascetin, H. Haznedaroglu and A.Y. Erkol, *Appl. Radiat. Isot*., **59**, 5 (2003).
17. B.J. Gao, F.Q. An and K.K. Liu, *Appl. Surf. Sci*., **253**, 1946 (2006).
18. A. Rahmani, H.Z. Mousavi and M. Fazli, *Desalination*, **253**, 94 (2010).
19. M.E. Mahmoud, M.M. Osman, O.F. Hafez, A.H. Hegazi and E. Elmelegy, *Desalination*, **251**, 123 (2010).
20. N.M. Wu and Z.K. Li, *Chem. Eng. J*., **215-216**, 894 (2013).
21. K. Kesenci, R. Say and A. Denizli, *Eur. Polym. J*., **38**, 1443 (2002).
22. A. Kara, L. Uzun, N. Besirli and A. Denizli, *J. Hazard. Mater*., **106**, 93 (2004).
23. Z.M. Jiang, L. Lv, W.M. Zhang, Q. Du, B.C. Pan, L. Yang and Q.X. Zhang, *Water Res*., **45**, 2191 (2011).
24. S.L. Xiao, H. Ma, M.W. Shen, S.Y. Wang, Q.G. Huang and X.Y. Shi, *Colloids Surf. A*, **381**, 48 (2011).
25. Z. Zhang, H. Zhang, Y. Hu, X. Yang and S. Yao, *Talanta*, **82**, 304 (2010).
26. Y.C. Lee and J.W. Yang, *J. Ind. Eng. Chem*., **18**, 1178 (2012).
27. L.Y. Hao, H.J. Song, L.C. Zhang, X.Y. Wan, Y.R. Tang and Y. Lv, *J. Colloid Interf. Sci*., **369**, 381 (2012).
28. Z.J. Li, F. Chen, L.Y. Yuan, Y.L. Liu, Y.L. Zhao, Z.F. Chai and W.Q. Shi, *Chem. Eng. J*., **210**, 539 (2012).
29. C.J. Madadrang, H.Y. Kim, G. Gao, N. Wang, J. Zhu, H. Feng, M. Gorring, M.L. Kasner and S. Hou, *ACS Appl. Mater. Interfaces*, **4**, 1186 (2012).
30. S.T. Yang, Y.L. Chang, H.F. Wang, G.B. Liu, S. Chen, Y.W. Wang, Y.F. Liu and A.N. Cao, *J. Colloid Interf. Sci*., **351**, 122 (2010).
31. X.J. Deng, L.L. Lü, H.W. Li and F. Luo, *J. Hazard. Mater*., **183**, 923 (2010).
32. V. Chandra, J. Park, Y. Chun, J.W. Lee, I.C. Hwang and K.S. Kim, *ACS Nano*, **4**, 3979 (2010).
33. X.Y. Yuan, Y.F. Wang, J. Wang, C. Zhou, Q. Tang and X.B. Rao, *Chem. Eng. J*., **221**, 204 (2013).
34. Y.Q. He, N.N. Zhang and X.D. Wang, *Chin. Chem. Lett*., **22**, 859 (2011).
35. G.X. Zhao, J.X. Li, X.M. Ren, C.L. Chen and X.K. Wang, *Environ. Sci. Technol*., **45**, 10454 (2011).
36. Y.Q. Leng, W.L. Guo, S.N. Su, C.L. Yi and L.T. Xing, *Chem. Eng. J*., **211-212**, 406 (2012).
37. W.M. Algothmi, N.M. Bandaru, Y. Yu, J.G. Shapter and A.V. Ellis, *J. Colloid Interf. Sci*., **397**, 32 (2013).
38. T.S. Sreeprasad, S.M. Maliyekkal, K.P. Lisha and T. Pradeep, *J. Hazard. Mater*., **186**, 921 (2011).
39. C.F. Chang, Q.D. Truong and J.R. Chen, *Appl. Surf. Sci*., **264**, 329 (2013).
40. L.L. Fan, C.N. Luo, M. Sun, X.J. Li and H.M. Qiu, *Colloids Surf. B*, **103**, 523 (2013).
41. X. Mi, G.B. Huang, W.S. Xie, W. Wang, Y. Liu and J.P. Gao, *Carbon*, **50**, 4856 (2012).
42. J.F. Che, L.Y. Shen and Y.H. Xiao, *J. Mater. Chem*., **20**, 1722 (2010).
43. L.J. Cote, F. Kim and J. Huang, *J. Am. Chem. Soc*., **131**, 1043 (2009).
44. A. Lerf, H.Y. He, M. Forster and J. Klinowski, *J. Phys. Chem. B*, **102**, 4477 (1998).
45. K. Krishnamoorthy, M. Veerapandian, R. Mohan and S.J. Kim, *Appl. Phys. A, Mater. Sci. Process*., **106**, 501 (2012).
46. Y.Q. Xiong, Y.Y. Xie, F. Zhang, E.C. Ou, Z.J. Jiang, L.L. Ke, D. Hu and W.J. Xu, *Mater. Sci. Eng. B*, **177**, 1163 (2012).
47. H.B. Li, L. Zou, L.K. Pan and Z. Sun, *Sep. Purif. Technol*., **75**, 8 (2010).
48. R.S. Juang and H.J. Shao, *Water Res*., **36**, 2999 (2002).
49. L. Bai, H. Hu, W. Fu, J. Wan, X. Cheng, L. Zhuge, L. Xiong and Q. Chen, *J. Hazard. Mater*., **195**, 261 (2011).
50. S. Lagergren and K.S. Vetenskapsakad, *Handl.*, **24**, 1 (1898).
51. Y.S. Ho and G. McKay, *Chem. Eng. J*., **70**, 115 (1998).
52. V.C. Taty-Costodes, H. Fauduet, C. Porte and A. Delacroix, *J. Hazard. Mater*., **105**, 121 (2003).
53. I. Langmuir, *J. Am. Chem. Soc*., **40**, 1361 (1918).
54. H. Freundlich, *Z. Phys. Chem*., **57**, 385 (1907).